Letter

Adiabatic expansion cooling of antihydrogen

M. Ahmadi,[1] B. X. R. Alves,[2] C. J. Baker,[3] W. Bertsche,[4,5,*] A. Capra,[6] S. Cohen,[7] C. Torkzaban,[8] C. L. Cesar,[9] M. Charlton,[3] R. Collister,[6] S. Eriksson,[3] A. Evans,[10,11] N. Evetts,[11] J. Fajans,[8,†] T. Friesen,[10,2] M. C. Fujiwara,[6] P. Granum,[2] J. S. Hangst,[2] M. E. Hayden,[12] D. Hodgkinson,[4,8,‡] C. A. Isaac,[3] M. A. Johnson,[4,5] S. A. Jones,[3,13] S. Jonsell,[14] N. Kalem,[8] N. Madsen,[3] D. Maxwell,[3] J. T. K. McKenna,[6,2,4] S. Menary,[15] T. Momose,[11,6] J. Munich,[12] K. Olchanski,[6] A. Olin,[6,16] P. Pusa,[1] C. Ø. Rasmussen,[2,17] F. Robicheaux,[18] R. L. Sacramento,[9] M. Sameed,[4,17] E. Sarid,[19,7] D. M. Silveira,[9] C. So,[10,6] G. Stutter,[2] T. D. Tharp,[20] R. I. Thompson,[10,6] D. P. van der Werf,[3] and J. S. Wurtele[8]
(The ALPHA Collaboration)

[1]*Department of Physics, University of Liverpool, Liverpool L3 5TR, United Kingdom*
[2]*Department of Physics and Astronomy, Aarhus University, DK-8000 Aarhus C, Denmark*
[3]*Department of Physics, Faculty of Science and Engineering, Swansea University, Swansea SA2 8PP, United Kingdom*
[4]*School of Physics and Astronomy, University of Manchester, Manchester M13 9PL, United Kingdom*
[5]*Cockcroft Institute, Sci-Tech Daresbury, Warrington WA4 4AD, United Kingdom*
[6]*TRIUMF, 4004 Wesbrook Mall, Vancouver, British Columbia, Canada V6T 2A3*
[7]*Department of Physics, Ben Gurion University, Beer Sheva 8410501, Israel*
[8]*Department of Physics, University of California at Berkeley, Berkeley, California 94720-7300, USA*
[9]*Instituto de Física, Universidade Federal do Rio de Janeiro, Rio de Janeiro 21941-972, Brazil*
[10]*Department of Physics and Astronomy, University of Calgary, Calgary, Alberta, Canada T2N 1N4*
[11]*Department of Physics and Astronomy, University of British Columbia, Vancouver, British Columbia, Canada V6T 1Z1*
[12]*Department of Physics, Simon Fraser University, Burnaby, British Columbia, Canada V5A 1S6*
[13]*Van Swinderen Institute for Particle Physics and Gravity, University of Groningen, NL-9747 AG Groningen, The Netherlands*
[14]*Department of Physics, Stockholm University, SE-10691 Stockholm, Sweden*
[15]*Department of Physics and Astronomy, York University, Toronto, Ontario, Canada M3J 1P3*
[16]*Department of Physics and Astronomy, University of Victoria, Victoria, British Columbia, Canada V8P 5C2*
[17]*CERN, Experimental Physics Department, CH-1211 Genève 23, Switzerland*
[18]*Department of Physics and Astronomy, Purdue University, West Lafayette, Indiana 47907, USA*
[19]*Soreq NRC, Yavne 81800, Israel*
[20]*Physics Department, Marquette University, P.O. Box 1881, Milwaukee, Wisconsin 53201-1881, USA*

(Received 10 May 2024; accepted 18 July 2024; published 16 September 2024)

Magnetically trapped antihydrogen atoms can be cooled by expanding the volume of the trap in which they are confined. We report a proof-of-principle experiment in which antiatoms are deliberately released from expanded and static traps. Antiatoms escape at an average trap depth of 0.08 ± 0.01 K (statistical errors only) from the expanded trap while they escape at average depths of 0.22 ± 0.01 and 0.17 ± 0.01 K from two different static traps. (We employ temperature-equivalent energy units.) Detailed simulations qualitatively agree with the escape times measured in the experiment and show a decrease of 38% (statistical error $< 0.2\%$) in the mean energy of the population after the trap expansion without significantly increasing antiatom loss compared to typical static confinement protocols. This change is bracketed by the predictions of one-dimensional and three-dimensional semianalytic adiabatic expansion models. These experimental, simulational, and model results are consistent with obtaining an adiabatically cooled population of antihydrogen atoms that partially exchanged energy between axial and transverse degrees of freedom during the trap expansion. This result is important for future antihydrogen gravitational experiments which rely on adiabatic cooling, and it will enable antihydrogen cooling beyond the fundamental limits of laser cooling.

DOI: 10.1103/PhysRevResearch.6.L032065

Adiabatic manipulations have been demonstrated in neutral atom trapping, for example, in Bose-Einstein condensation where adiabatic compression increases collision rates prior to evaporative cooling [1], in optical lattices [2,3], and in ultracold neutron trapping where adiabatic cooling during

*Contact author: william.bertsche@manchester.ac.uk
†Contact author: joelfajans@gmail.com
‡Contact author: danielle.louise.hodgkinson@cern.ch

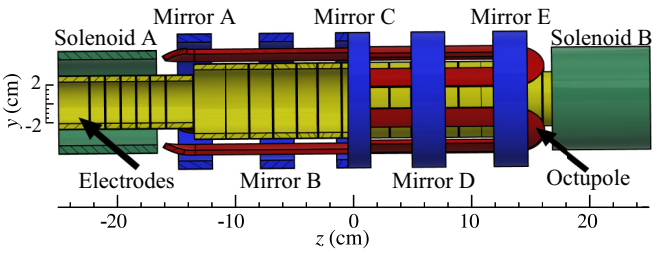

FIG. 1. The ALPHA-2 apparatus. Penning-Malmberg trap electrodes (yellow) confine antiprotons and positrons axially. Ioffe-Pritchard trap magnets: Mirrors A–E (blue), octupole (red), and solenoids A and B (green). A silicon vertex detector (SVD) (not shown) surrounds these magnets and counts $\overline{\mathrm{H}}$ annihilating when escaping the trap. A 1-T solenoid (not shown) produces a uniform axial magnetic field over this whole region, and surrounds the SVD. The radius-to-length scale is increased for clarity.

magnetic trap filling can increase the number of stored neutrons [4]. The temperature of charged plasmas, including antimatter plasmas of antiprotons [5] and positrons [6], is routinely reduced via adiabatic manipulations of electric potentials [7]. In this Letter, we demonstrate adiabatic expansion cooling of antimatter atoms.

The ALPHA collaboration at CERN studies the fundamental properties of antihydrogen ($\overline{\mathrm{H}}$) atoms [8–11]; all such properties can be better measured with colder antiatoms. Although adiabatic expansion does not result in phase-space cooling, it does reduce velocity which is beneficial in these experiments. For instance, the precision of $\overline{\mathrm{H}}$ spectroscopy measurements will improve by reducing the $\overline{\mathrm{H}}$ velocity parallel and perpendicular to the spectroscopy laser beam, thereby suppressing Doppler broadening [8,9], and transit-time broadening [10], respectively. Lower $\overline{\mathrm{H}}$ energies permit atom confinement in shallower traps, which will increase the sensitivity of measurements of the charge neutrality [11] and gravitational interactions [12] of $\overline{\mathrm{H}}$. In addition, $\overline{\mathrm{H}}$ could be laser cooled [13] in a small magnetic volume, and then adiabatic expansion cooled, yielding lower-energy $\overline{\mathrm{H}}$ than can be obtained with either technique individually.

For this study, $\overline{\mathrm{H}}$ was produced by combining antiproton and positron plasmas, confined in adjacent Penning-Malmberg wells [14]. The resultant $\overline{\mathrm{H}}$ is confined in a superimposed Ioffe-Pritchard trap (Fig. 1); the required radial magnetic minimum is created by an octupole magnet while the axial minimum is created by a set of five axially spaced mirror coils and two end solenoids. Low-field-seeking ground-state $\overline{\mathrm{H}}$'s are confined in a potential,

$$U(\mathbf{x},t) = \mu_B(|\mathbf{B}(\mathbf{x},t)| - |\mathbf{B}(\mathbf{x}_{\min},t)|), \tag{1}$$

and experience a force $m\ddot{\mathbf{x}} = -\nabla U$, where $\mathbf{B}(\mathbf{x},t)$ is the magnetic field, μ_B is the Bohr magneton, m is the $\overline{\mathrm{H}}$ mass, and $\mathbf{x}_{\min}$ is the location of the minimum magnetic potential within the trap volume. This potential confines $\overline{\mathrm{H}}$ with energy below the magnetic potential depth of approximately 0.5 K. We use temperature-equivalent energy units in this Letter, i.e., $T = U/k_B$, where k_B is the Boltzmann constant.

When confined in the magnetic potential, an $\overline{\mathrm{H}}$'s phase-space volume is conserved if $U(\mathbf{x},t)$ is changed slowly, i.e., if

$$\tau_{\mathrm{bounce}} \frac{d}{dt} U(\mathbf{x},t) \ll U(\mathbf{x},t), \tag{2}$$

where $\tau_{\mathrm{bounce}} \sim 10$ ms is the typical duration of an axial transit for an uncooled $\overline{\mathrm{H}}$. When this condition is met, an $\overline{\mathrm{H}}$'s energy should decrease as its trapping volume and associated trajectory lengths increase, thereby achieving adiabatic expansion cooling.

Generally, the extent of overall energy decrease depends on the coupling between degrees of freedom. In many systems, collisions couple particle degrees of freedom, so adiabatically cooling one dimension can cool in all dimensions [5]. In the ALPHA experiment, however, the extremely low density of trapped $\overline{\mathrm{H}}$ ($\sim$1 atom per cubic centimeter) and the extremely good ($<10^{-14}$ mbar) vacuum conditions reduce collisions to a negligible level [15]. As a result, any energy mixing between dimensions must be caused by single-particle orbit trajectory dynamics due to details of the magnetic field gradients in the trap [16].

After performing our expansion technique, we deliberately release trapped $\overline{\mathrm{H}}$ populations, resulting in annihilations that can be resolved in time and compared to detailed trajectory simulations. In this Letter, we show that simulated and experimental annihilation-time distributions agree qualitatively, and consequently, we can infer the $\overline{\mathrm{H}}$ energy from these simulations. Further, we present calculations using two semianalytic adiabatic models which make limiting assumptions about the exchange of energies between degrees of freedom. These calculations bound the simulated energy decrease and show that the experimental and simulational results are consistent with adiabatic cooling of an $\overline{\mathrm{H}}$ population that partially exchanges axial and transverse energy components during the expansion.

For this study, we conducted three interleaved experimental trials in which we released a population of $\overline{\mathrm{H}}$: ($\mathcal{A}$) after an axial adiabatic expansion, ($\mathcal{B}$) after a hold in the initial, unexpanded trap, and ($\mathcal{C}$) after a hold in a static trap nearly identical to the final state of ($\mathcal{A}$). Figure 2 shows the time evolution of the on-axis magnetic potential for each trial from $\overline{\mathrm{H}}$ formation at $t < -24$ s up to the onset of trap release at $t = 0$ s. Each trial consisted of ramping to the trial's initial magnetic trapping potential, forming $\overline{\mathrm{H}}$, then waiting 1 s before ramping solenoid A (which was used to increase the magnetic field in the particle preparation region) from full field to zero field in 5 s. Due to details of the Penning-Malmberg trap geometry, the center of $\overline{\mathrm{H}}$ formation is limited to discrete axial locations. For trial $\mathcal{A}$, the initial well was a short magnetic trap between mirrors A and C, with D and E also energized, resulting in a trap depth of 0.48 K. $\overline{\mathrm{H}}$ was formed as close to the trap minimum as possible (Fig. 2) at a magnetic potential $\sim$0.03 K above the bottom of the trap. After $\overline{\mathrm{H}}$ formation, first mirror C and then mirror D were linearly deenergized to cause a largely axial trap expansion over $\sim$24 s. (There was also a small amount of unavoidable radial compression in this trial.) Trial $\mathcal{B}$ formed $\overline{\mathrm{H}}$ in the same initial trapping potential as trial $\mathcal{A}$, but left the potential largely fixed for $\sim$24 s. Trial $\mathcal{C}$ mimicked $\overline{\mathrm{H}}$ production and trapping typical of the ALPHA spectroscopy experiments conducted in Ref. [14]; this involved energizing mirror B with a small negative

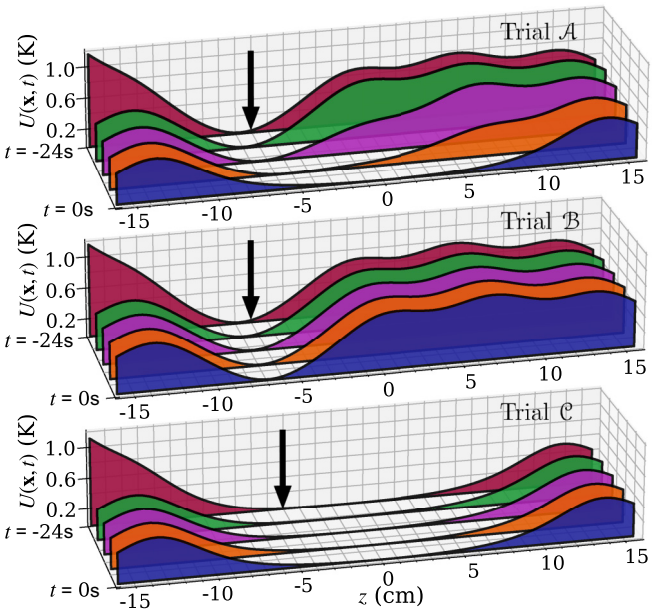

FIG. 2. On-axis ($r = 0$) magnetic potential, $U(\mathbf{x}, t)$, at five equally spaced times (different colors) from $t = -24$ s to the start of the octupole ramp-down at $t = 0$ s during adiabatic expansion trial $\mathcal{A}$, control trial $\mathcal{B}$, and control trial $\mathcal{C}$. Antihydrogen is formed at $t < -24$ s, centered at the location indicated by the black arrow.

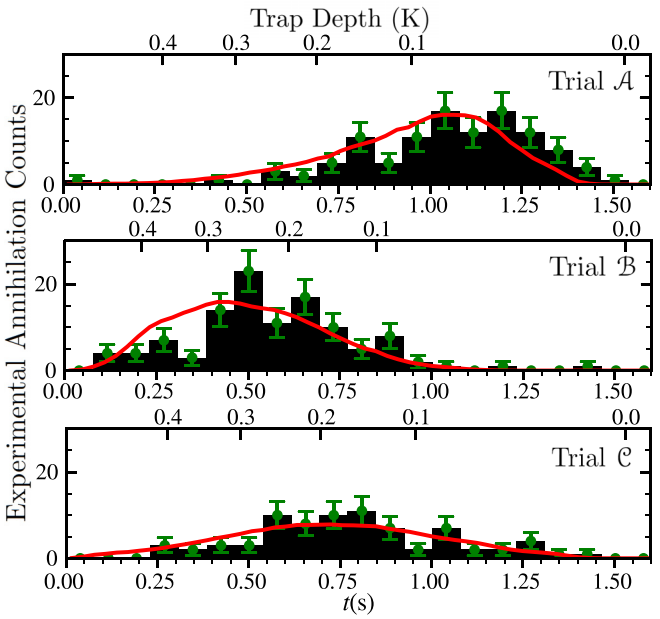

FIG. 3. Annihilation-time histograms (black bars) during octupole ramp-down for the three experimental trials: Adiabatic expansion trial $\mathcal{A}$ (111 counts), control trial $\mathcal{B}$ (112 counts), and control trial $\mathcal{C}$ (77 counts). The upper x axis is the depth of the magnetic trapping potential at the time on the lower x axis for each trial (note that this mapping is monotonic, but nonlinear and is different for $\mathcal{B}$ compared to $\mathcal{A}$ and $\mathcal{C}$ due to the difference in trapping potential at $t = 0$ s). The red line shows the simulated annihilation time distribution for each trial, normalized to the area of the experimental annihilation histogram. Total simulated counts (that survive until $t = 0$ s) for trials $\mathcal{A}$, $\mathcal{B}$, and $\mathcal{C}$ are 179 631, 180 553, and 175 399, respectively. Green error bars are standard counting errors for the experimental data; similar error bars are not visible on this scale for the simulated data.

current, resulting in a total trap depth of 0.49 K, and initializing $\overline{\mathrm{H}}$ at a different location (Fig. 2) at an on-axis potential of ∼0.01 K. Mirror B was then linearly deenergized over the course of trial $\mathcal{C}$ to release $\overline{\mathrm{H}}$ from the same postexpansion potential of trial $\mathcal{A}$. During the expansion or control hold for each trial, changes in trap depth were negligible (<0.02 K).

After expanding or holding, we linearly ramped the octupole from its full field to zero field from $t = 0$ s to $t \approx 1.5$ s in all trials, causing all remaining antiatoms to annihilate on the trap walls. $\overline{\mathrm{H}}$ annihilation events were identified through analysis of events from ALPHA's silicon vertex detector [17,18] and recorded with a time uncertainty of ∼2 μs. Annihilation counts presented here have not been scaled by detector efficiency ($67.6 \pm 0.3\%$) nor corrected for cosmic background counts (53 ± 4) × 10^{-3} s^{-1}.

Each trial was conducted 13 times. Figure 3 shows the annihilation-time histograms during the octupole ramp-down for each trial. Because the trap depth decreases monotonically during this operation, $\overline{\mathrm{H}}$ annihilation time here serves as an imprecise energy diagnostic by establishing a lower bound on the energy of each released antiatom. The average magnetic trap depth at the time of annihilation for trial $\mathcal{A}$ events is 0.08 ± 0.01 K, compared to 0.22 ± 0.01 and 0.17 ± 0.01 K (statistical errors only) for trials $\mathcal{B}$ and $\mathcal{C}$, respectively, meaning the $\overline{\mathrm{H}}$ subject to the adiabatic cooling protocol have less energy at the end than those of the control trials.

We simulate $\overline{\mathrm{H}}$ trajectories using methods similar to Ref. [16]. A second-order symplectic Leapfrog integrator with a fixed 3.5 μs time step gives the solution to the $\overline{\mathrm{H}}$ equations of motion. The fields from the mirror coils and octupole are calculated using approximate analytic models [19], and the field from solenoid A is given by an off-axis expansion method [20]. Initial antiatom positions are randomly sampled from an ellipsoidal uniform distribution of length 10 mm and radius 0.8 mm centered at the locations shown in Fig. 2 and mimicking the positron plasma spatial distribution. $\overline{\mathrm{H}}$ velocity is sampled from a thermal distribution with temperature 50 K. Antiatoms are initialized in high principal quantum number states and allowed to cascade to the ground state through circular transitions as in Ref. [21]. Of 200 000 antiatoms remaining after 1 s, in the smaller initial trap volume of trials $\mathcal{A}$ and $\mathcal{B}$, ∼85% have energy less than the trap depth, while the remaining ∼15%, known as quasitrapped antiatoms [22,23], are confined with total energy greater than the trap depth. For the larger initial potential of trial $\mathcal{C}$, the number of quasitrapped antiatoms is ∼20%.

The simulated annihilation-time distributions of the three experimental trials during the octupole ramp-down, shown in red in Fig. 3, are in qualitative agreement with the experimental data. The average magnetic trap depth at the simulated annihilation time is 0.11 K for trial $\mathcal{A}$, compared to 0.25 and 0.20 K for trials $\mathcal{B}$ and $\mathcal{C}$, respectively (statistical errors < 0.001 K), which are similar to the equivalent quantities calculated using the experimental annihilation times. The simulations predict 10.2%, 9.7%, and 12.3% of the $\overline{\mathrm{H}}$ population remaining after 1 s annihilate during the expansion or hold period in trials $\mathcal{A}$, $\mathcal{B}$, and $\mathcal{C}$, respectively. In

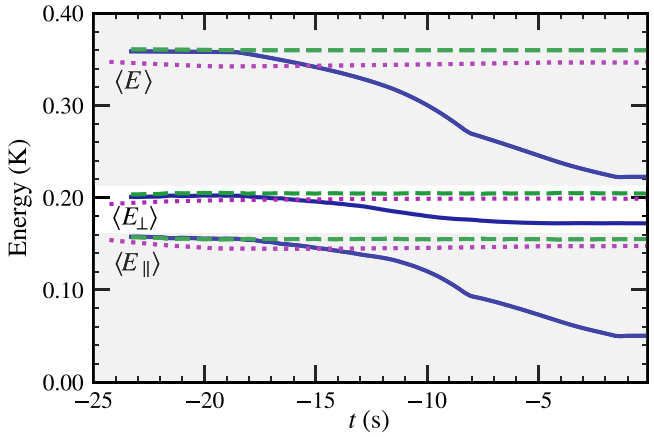

FIG. 4. Ensemble-averaged total energy $\langle E\rangle$ (top curve set), transverse energy $\langle E_\perp\rangle$ (middle curve set), and axial energy $\langle E_\parallel\rangle$ (bottom curve set), for simulated $\overline{\mathrm{H}}$ trajectories as a function of time relative to the start of the octupole ramp-down ($t = 0$ s) for trials $\mathcal{A}$ (solid blue), $\mathcal{B}$ (dashed green), and $\mathcal{C}$ (dotted magenta).

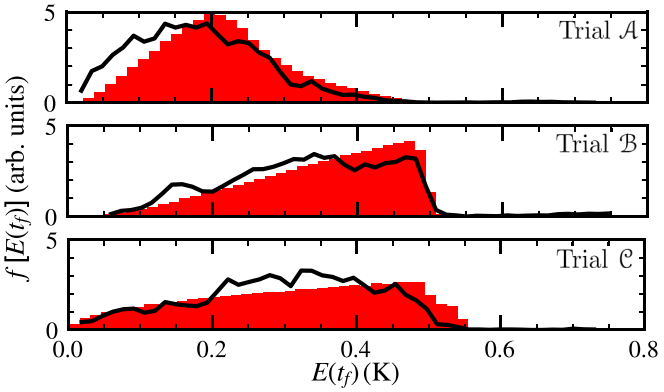

FIG. 5. Energy distribution function $f[E(t_f)]$ just prior to octupole ramp-down at $t_f \approx -50$ ms sampled from the simulation (red histogram) and reconstructed (see text) from experimental annihilation times (black solid curve) for trials $\mathcal{A}$, $\mathcal{B}$, and $\mathcal{C}$. The area of each distribution is normalized to 1.

the equivalent experimental period, we observe no excess of counts during trial $\mathcal{A}$ compared to trials $\mathcal{B}$ and $\mathcal{C}$. In addition, we observe no significant difference in the number of experimental counts for $t > 0$ s in trials $\mathcal{A}$ and $\mathcal{B}$ (in which $\overline{\mathrm{H}}$ was formed in the same magnetic potential). As a result, loss of high-energy quasitrapped $\overline{\mathrm{H}}$ does not contribute significantly to the difference in average magnetic trap depth at annihilation time in the three trials.

We determine the simulated antiatoms' axial, $E_\parallel$, and transverse, $E_\perp$, energy components when they cross the axial magnetic minimum as in Ref. [16]. The total energy is $E = E_\perp + E_\parallel$. Figure 4 shows the time evolution of the ensemble means of these energy components ($\langle E\rangle$, $\langle E_\parallel\rangle$, $\langle E_\perp\rangle$) up to the octupole ramp-down at $t = 0$ s. Simulated antiatoms that escape before $t = 0$ s are excluded from the means to remove the effect of any energy decrease due to the loss of high-energy quasitrapped antiatoms, thus isolating the effect of adiabatic changes in mean energy. In the simulation of adiabatic expansion trial $\mathcal{A}$, $\langle E\rangle$ decreased by 38%, $\langle E_\parallel\rangle$ decreased by 68%, and $\langle E_\perp\rangle$ decreased (due to energy mixing) by 14% (statistical errors all <0.2%). The component means $\langle E_\parallel\rangle$ and $\langle E_\perp\rangle$ do not equally reduce, showing that the antiatoms' degrees of freedom are not equilibrated at the end of the expansion. These values remained nearly constant throughout trials $\mathcal{B}$ and $\mathcal{C}$, but the small shifts observed are consistent with adiabatic changes due to the minor magnet ramps that occurred (see earlier text). The simulated energy decrease in trial $\mathcal{A}$ is less than would be estimated by comparing the average magnetic trap depths at annihilation time for trials $\mathcal{A}$ and $\mathcal{B}$ since annihilation time in this experiment is significantly correlated with both $E_\parallel$ and $E_\perp$ due to a combination of adiabatic cooling, energy mixing, and details of the changing magnetic fields, all taking place during the ramp-down as detailed in Ref. [24].

Just prior to the octupole ramp-down ($t_f \approx -50$ ms), the distributions of total energy for the simulated antiatoms, $f[E(t_f)]$, shown in Fig. 5, have means of 0.22, 0.36, and 0.35 K (statistical errors < 0.0003 K) for trials $\mathcal{A}$, $\mathcal{B}$, and $\mathcal{C}$, respectively. We employ the method developed in Ref. [19] to reconstruct the $f[E(t_f)]$ that is most consistent with the observed experimental annihilation-time distribution, $f(t_a)$, by performing the integral $f[E(t_f)] = \int_0^\infty P[E(t_f|t_a)]f(t_a)dt_a$, where $P[E(t_f|t_a)]$ is the probability for an antiatom to have energy $E(t_f)$ given that it is annihilated at t_a. The integral is approximated by randomly sampling 100 simulated counts within 50 ms of an experimental t_a; the $E(t_f)$ of the sampled counts for all experimental t_a are aggregated to form $f[E(t_f)]$. The respective reconstructed means are 0.18 ± 0.01, 0.33 ± 0.01, and 0.30 ± 0.01 K (statistical errors only), showing that, under the assumption that the experimental and simulated $P[E(t_f|t_a)]$ is the same, the experimentally observed annihilation distribution is consistent with a similar degree of energy reduction as in the simulations.

We have also compared the simulation results against semianalytic adiabatic expansion models which assume that Eq. (2) is satisfied, that the adiabatic invariant $I = \oint \mathbf{p}\cdot\mathbf{dl}$ (where $\mathbf{p}$ is the antiatom momentum and $\mathbf{dl}$ is the infinitesimal change in trajectory length) is conserved for closed orbits, and that the orbits are periodic when decomposed into orthogonal coordinates. We can then separate the adiabatic invariant into components such as $I_z = \oint p_z(z)\,dz$, that can be calculated for an antiatom's orbit between consecutive crossings of the transverse midplane of the magnetic potential. Under the assumption that the trap potential changes size in the axial direction only (broadly the case for trial $\mathcal{A}$), and assuming that only axial momentum is affected by this, we have model 1,

$$I^2 \propto E_\parallel(t)\{L_z[t; E(t)]\}^2 = \text{const}, \tag{3}$$

where $L_z[t; E_\parallel(t)]$ is the axial trap length accessible by an antiatom of axial energy $E_\parallel(t)$ at time t. Assuming some process fully equilibrates energy between antiatom degrees of freedom in all directions during the trap expansion and trajectory ergodicity leads to model 2,

$$I^2 \propto E(t)\{V[t; E(t)]\}^{\frac{2}{3}} = \text{const}, \tag{4}$$

where $V[t; E(t)]$ is the volume that is energetically accessible to an antiatom with total energy $E(t)$. Equation (4) is derived in Ref. [24] and is equivalent to the ergodic adiabatic invariant applied to chaotic systems in Ref. [25]. We expect

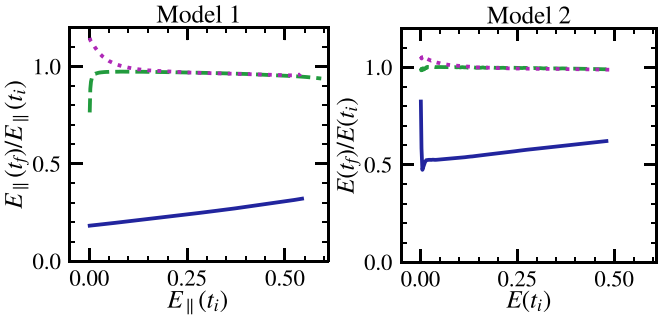

FIG. 6. Fractional change in energy predicted by adiabatic models 1 and 2 as a function of initial energy for trials $\mathcal{A}$ (solid blue), $\mathcal{B}$ (dashed green), and $\mathcal{C}$ (dotted magenta). Energies are plotted up to the on-axis trap depth at t_i for model 1 and the total trap depth at t_i for model 2. The low-energy features in model 2 for trial $\mathcal{A}$ are due to the initial magnetic trapping volume being toroidal for energies $\lesssim$10 mK (see Refs. [16,24]) and are expected to have little influence on the distributions discussed here.

[16] that, due to the complex trajectories in our magnetic potential, energy exchange should be bracketed by these two models.

We employ a fixed-point iterative method to solve for the model predictions of the antiatom energy at t_f given the energy at t_i. For model 1, the iteration equation is

$$E_{\parallel,k+1}(t_f) = E_\parallel(t_i)\left(\frac{L_z\left[t_i; E_\parallel(t_i)\right]}{L_z\left[t_f; E_{\parallel,k}(t_f)\right]}\right)^2, \tag{5}$$

where the subscript k is the iteration step number. [Note that k does not represent any physical parameter; it indexes steps towards the converged numeric solutions for $E_\parallel(t_f)$.] An equivalent method is used to calculate $E(t_f)$ from model 2. $L_z(t, E_\parallel)$ and $V(t, E)$ are calculated numerically using $U(\mathbf{x}, t)$. We approximate $L_z(t, E_\parallel)$ as the on-axis trap length energetically accessible to an antiatom initialized at the axial magnetic minimum with axial energy $E_\parallel$. The solutions to Eq. (5) (and the model 2 equivalent) are shown in Fig. 6.

Drawing the energy at t_i from the simulation, we evaluate the model-predicted change in energy for each simulated antiatom. Table I shows the ratios of final to initial $\langle E\rangle$, $\langle E_\parallel\rangle$, and $\langle E_\perp\rangle$ predicted by the two models as well as the full simulation results for adiabatic expansion trial $\mathcal{A}$. Model 1 assumes no energy exchange between axial and transverse motion, whereas model 2 assumes full energy equilibration during the expansion. In model 2 there is a smaller decrease in axial energy (compared to model 1) and a significant decrease in transverse energy. The trial A simulated energy decreases lie between the model results, consistent with an adiabatic process in which there is partial energy mixing between degrees of freedom as is predicted by simulation (see Ref. [16]).

In conclusion, we have demonstrated adiabatic cooling of $\overline{\mathrm{H}}$ atoms confined within the ALPHA neutral atom traps. We have shown that the experimentally observed annihilation-time distributions are qualitatively consistent with simulations, which predict a 38% total energy decrease with a 68% decrease in axial energy (statistical errors $< 0.2\%$) resulting from adiabatic cooling.

TABLE I. Percent change of ensemble-averaged energies for the trial $\mathcal{A}$ simulation and the two adiabatic models (1 and 2) from the start to the end of the expansion. All errors on the ratios propagated from the standard error on the means are <0.2%.

	$\frac{\langle E(t_f)\rangle}{\langle E(t_i)\rangle}$ (%)	$\frac{\langle E_\parallel(t_f)\rangle}{\langle E_\parallel(t_i)\rangle}$ (%)	$\frac{\langle E_\perp(t_f)\rangle}{\langle E_\perp(t_i)\rangle}$ (%)
Simulation	62	32	86
Model 1	66	24	100
Model 2	60	45	71

Beyond cooling, the simulations and the experimental data demonstrated here increase confidence in the use of the simulation in other contexts to predict the details of the $\overline{\mathrm{H}}$ orbit dynamics. Understanding these details will be necessary to fully analyze the experiments, and highlights the importance of planned future experiments to benchmark simulated $\overline{\mathrm{H}}$ energy mixing dynamics.

Larger changes in trap volume will result in greater cooling. For example, an additional radial adiabatic expansion could be achieved via slow manipulations of the octupole current. Since this process reduces the trap depth, cooling is limited by the antiatom loss that can be tolerated. Following laser cooling of an $\overline{\mathrm{H}}$ population in a well similar to the trial $\mathcal{A}$ initial well to $\langle E\rangle \approx 0.05$ K, simulation results (not presented here) predict that a combined axial and radial expansion procedure would reduce $\langle E\rangle$ by 74% with around 23% antiatom loss; this procedure is predicted to result in significantly more transverse energy reduction, with $\langle E_\parallel\rangle$ and $\langle E_\perp\rangle$ reducing by 77% and 73%, respectively. By enabling cooling beyond the fundamental limits of laser cooling, the work reported in this Letter provides a route to production of the lowest-energy antihydrogen atoms trapped to date.

This work was supported by the European Research Council through its Advanced Grant programme (J.S.H.); CNPq, FAPERJ, RENAFAE (Brazil); NSERC, NRC/TRIUMF, EHPDS/EHDRS, FQRNT (Canada); FNU (Nice Centre), Carlsberg Foundation (Denmark); JSPS Postdoctoral Fellowships for Research Abroad (Japan); ISF (Israel); EPSRC, STFC, the Royal Society and the Leverhulme Trust (U.K.); DOE, NSF (U.S.); and VR (Sweden). We thank A. Zhong, E. Thorpe-Woods, and A. Christensen for useful discussions.

Experimental data was obtained using the ALPHA-2 antihydrogen trapping apparatus, which was designed, constructed and operated by the ALPHA Collaboration. J.F. conceptualized the work. W.B., J.F. and D.M. led the experimental campaign. J.T.K.M., A.C., and K.O. analyzed the detector data. The antihydrogen dynamics were modeled and compared with data using a simulation developed by D.H., J.T.K.M., W.B., P.G., J.F. and F.R. Implementation and simulations of the experimental procedure were performed by D.H.; N.K. performed simulations of optimized adiabatic cooling protocols. S.J. and D.H. performed calculations of collisions on background gases. The manuscript was written by D.H. and W.B., initially edited and improved by J.F. and J.S.W., and further edited and improved by the entire author list. D.H. is the corresponding author.

[1] K. B. Davis, M.-O. Mewes, M. R. Andrews, N. J. van Druten, D. S. Durfee, D. M. Kurn, and W. Ketterle, Bose-Einstein condensation in a gas of sodium atoms, Phys. Rev. Lett. **75**, 3969 (1995).

[2] J. Chen, J. G. Story, J. J. Tollett, and R. G. Hulet, Adiabatic cooling of atoms by an intense standing wave, Phys. Rev. Lett. **69**, 1344 (1992).

[3] A. Kastberg, W. D. Phillips, S. L. Rolston, R. J. C. Spreeuw, and P. S. Jessen, Adiabatic cooling of cesium to 700 nK in an optical lattice, Phys. Rev. Lett. **74**, 1542 (1995).

[4] A. Andreev, A. Glushkov, P. Geltenbort, V. Ezhov, V. Knyaz'kov, G. Krygin, and V. Ryabov, Ultracold neutron cooling upon reflection from a moving wall, Tech. Phys. Lett. **39**, 370 (2013).

[5] G. Gabrielse, W. S. Kolthammer, R. McConnell, P. Richerme, R. Kalra, E. Novitski, D. Grzonka, W. Oelert, T. Sefzick, M. Zielinski *et al.*, Adiabatic cooling of antiprotons, Phys. Rev. Lett. **106**, 073002 (2011).

[6] C. J. Baker, W. Bertsche, A. Capra, C. L. Cesar, M. Charlton, A. C. Mathad, S. Eriksson, A. Evans, N. Evetts, S. Fabbri *et al.*, Sympathetic cooling of positrons to cryogenic temperatures for antihydrogen production, Nat. Commun. **12**, 6139 (2021).

[7] A. W. Hyatt, C. F. Driscoll, and J. H. Malmberg, Measurement of the anisotropic temperature relaxation rate in a pure electron plasma, Phys. Rev. Lett. **59**, 2975 (1987).

[8] M. Ahmadi, B. X. R. Alves, C. J. Baker, W. Bertsche, A. Capra, C. Carruth, C. L. Cesar, M. Charlton, S. Cohen, R. Collister *et al.*, Investigation of the fine structure of antihydrogen, Nature (London) **578**, 375 (2020).

[9] M. Ahmadi, B. X. R. Alves, C. J. Baker, W. Bertsche, A. Capra, C. Carruth, C. L. Cesar, M. Charlton, S. Cohen, R. Collister *et al.*, Observation of the 1S–2P Lyman-α transition in antihydrogen, Nature (London) **561**, 211 (2018).

[10] M. Ahmadi, B. X. R. Alves, C. J. Baker, W. Bertsche, A. Capra, C. Carruth, C. L. Cesar, M. Charlton, S. Cohen, R. Collister *et al.*, Characterization of the 1S-2S transition in antihydrogen, Nature (London) **557**, 71 (2018).

[11] M. Ahmadi, M. Baquero-Ruiz, W. Bertsche, E. Butler, A. Capra, C. Carruth, C. L. Cesar, M. Charlton, A. E. Charman, S. Eriksson *et al.*, An improved limit on the charge of antihydrogen from stochastic acceleration, Nature (London) **529**, 373 (2016).

[12] E. K. Anderson, C. J. Baker, W. Bertsche, N. M. Bhatt, G. Bonomi, A. Capra, I. Carli, C. L. Cesar, M. Charlton, A. Christensen *et al.*, Observation of the effect of gravity on the motion of antimatter, Nature (London) **621**, 716 (2023).

[13] C. J. Baker, W. Bertsche, A. Capra, C. Carruth, C. L. Cesar, M. Charlton, A. Christensen, R. Collister, A. C. Mathad *et al.*, Laser cooling of antihydrogen atoms, Nature (London) **592**, 35 (2021).

[14] M. Ahmadi, B. X. R. Alves, C. J. Baker, W. Bertsche, E. Butler, A. Capra, C. Carruth, C. L. Cesar, M. Charlton, S. Cohen *et al.*, Observation of the 1S-2S transition in trapped antihydrogen, Nature (London) **541**, 506 (2017).

[15] S. Jonsell, E. A. G. Armour, M. Plummer, Y. Liu, and A. C. Todd, Helium–antihydrogen scattering at low energies, New J. Phys. **14**, 035013 (2012).

[16] M. Zhong, J. Fajans, and A. F. Zukor, Axial to transverse energy mixing dynamics in octupole-based magnetostatic antihydrogen traps, New J. Phys. **20**, 053003 (2018).

[17] G. B. Andresen, M. D. Ashkezari, W. Bertsche, P. D. Bowe, E. Butler, C. L. Cesar, S. Chapman, M. Charlton, A. Deller, S. Eriksson *et al.*, Antihydrogen annihilation reconstruction with the ALPHA silicon detector, Nucl. Instrum. Methods Phys. Res. Sect. A **684**, 73 (2012).

[18] C. Amole, G. B. Andresen, M. D. Ashkezari, M. Baquero-Ruiz, W. Bertsche, C. Burrows, E. Butler, A. Capra, C. L. Cesar, S. Chapman *et al.*, Silicon vertex detector upgrade in the ALPHA experiment, Nucl. Instrum. Methods Phys. Res. Sect. A **732**, 134 (2013).

[19] C. Amole, G. Andresen, M. Ashkezari, M. Baquero-Ruiz, W. Bertsche, E. Butler, C. Cesar, S. Chapman, M. Charlton, A. Deller *et al.*, Discriminating between antihydrogen and mirror-trapped antiprotons in a minimum-B trap, New J. Phys. **14**, 015010 (2012).

[20] K. T. Mcdonald, Expansion of an axially symmetric, static magnetic field in terms of its axial field, http://kirkmcd.princeton.edu/examples/axial.pdf (2011) (unpublished).

[21] C. L. Taylor, J. Zhang, and F. Robicheaux, Cooling of Rydberg during radiative cascade, J. Phys. B: At., Mol., Opt. Phys. **39**, 4945 (2006).

[22] K. J. Coakley, M. S. Dewey, M. G. Huber, C. R. Huffer, P. R. Huffman, D. E. Marley, H. P. Mumm, C. M. O'Shaughnessy, K. W. Schelhammer, A. K. Thompson, and A. T. Yue, Survival analysis approach to account for non-exponential decay rate effects in lifetime experiments, Nucl. Instrum. Methods Phys. Res. Sect. A **813**, 84 (2016).

[23] G. B. Andresen, M. D. Ashkezari, M. Baquero-Ruiz, W. Bertsche, P. D. Bowe, E. Butler, C. L. Cesar, M. Charlton, A. Deller, S. Eriksson *et al.*, Confinement of antihydrogen for 1,000 seconds, Nat. Phys. **7**, 558 (2011).

[24] D. Hodgkinson, On the dynamics of adiabatically cooled antihydrogen in an octupole-based Ioffe-Pritchard magnetic trap, Ph.D. thesis, The University of Manchester, 2022.

[25] R. Brown, E. Ott, and C. Grebogi, Ergodic adiabatic invariants of chaotic systems, Phys. Rev. Lett. **59**, 1173 (1987).